Available online at www.sciencedirect.com
ScienceDirect
Journal of Solid State Chemistry 181 (2008) 628–636
JOURNAL OF SOLID STATE CHEMISTRY
www.elsevier.com/locate/jssc

Facile synthesis of multifunctional multiwalled carbon nanotubes/Fe_3O_4 nanoparticles/polyaniline composite nanotubes

Lirong Kong[a], Xiaofeng Lu[b], Wanjin Zhang[a,*]

[a]*Alan G. MacDiarmid Institute, Jilin University, Changchun 130012, PR China*
[b]*Department of Biomedical Engineering, Washington University, St Louis, MI 63130, USA*

Received 10 November 2007; received in revised form 27 December 2007; accepted 6 January 2008
Available online 10 January 2008

Abstract

With an average diameter of 100–150 nm, composite nanotubes of polyaniline (PANI)/multiwalled carbon nanotubes (MWNTs) containing Fe_3O_4 nanoparticles (NPs) were synthesized by a two-step method. First, we synthesized monodispersed Fe_3O_4 NPs ($d = 17.6$ nm, $\sigma = 1.92$ nm) on the surface of MWNTs and then decorated the nanocomposites with a PANI layer via a self-assembly method. SEM and TEM images indicated that the obtained samples had the morphologies of nanotubes. The molecular structure and composition of MWNTs/Fe_3O_4 NPs/PANI nanotubes were characterized by Fourier transform infrared spectra (FTIR), energy dispersive X-ray spectrometry (EDX), X-ray photoelectron spectra (XPS), X-ray diffraction (XRD) and Raman spectra. UV–vis spectra confirmed the existence of PANI and its response to acid and alkali. As a multifunctional material, the conductivity and magnetic properties of MWNTs/Fe_3O_4 NPs/PANI composites nanotubes were also investigated.

Keywords: Multiwalled carbon nanotubes; Iron oxide nanoparticles; Polyaniline; Nanocomposites

1. Introduction

Carbon nanotubes (CNTs), discovered by Iijima [1], have attracted more and more attention for their unique structure and excellent mechanical, electrical and thermal properties [2–5]. Due to their fascinating nanoscale dimensions and high surface areas, CNTs are considered as an ideal carrier to direct assembly of inorganic nanoparticles (NPs) which have special properties [6–12]. Among these inorganic NPs, iron oxide nanoparticles (Fe_3O_4 NPs) are of great importance for their good magnetic properties which endow them with potential applications in color imaging, magnetic recoding media, soft magnetic materials and ferrofluids [13]. On the other hand, polyaniline (PANI) is one of the most widely investigated conducting polymers because of its good processibility, environmental stability, and its oxidation or protonation-adjustable electro-optical properties as well as its potential applications in many fields [14–17]. Recently, one-dimensional (1D) nanostructures of PANI including nanowires, nanorods, and nanotubes have received great attention due to their unique properties [18–20]. In order to combine the advantages of multiwalled carbon nanotubes (MWNTs), Fe_3O_4 NPs and PANI, it is a method to prepare a new kind of composite containing such three kinds of materials.

As a matter of fact, several groups have done much work on synthesizing nanocomposites containing such two different nanoscale materials. Wan et al. reported the in situ decoration of carbon nanotubes with nearly monodispersed magnetite NPs [21], but their method need in situ high temperature decomposition of the iron precursor. Correa-Duarte et al. studied the alignment of carbon nanotubes under low magnetic fields through attachment of magnetic NPs [22]. They coated CNTs with magnetic NPs by combining the polymer wrapping and layer-by-layer assembly techniques. This method needs two steps including the preparation of Fe_3O_4 NPs first and then the wrapping process. On the other hand, PANI/magnetic NPs composite nanostrutures have also been widely studied in the past few years. Zhang et al. and Long et al. prepared

*Corresponding author. Fax: +86 431 85168924.
E-mail address: wjzhang@jlu.edu.cn (W. Zhang).

0022-4596/$ - see front matter © 2008 Elsevier Inc. All rights reserved.
doi:10.1016/j.jssc.2008.01.006

the composite nanostructures of PANI containing nanomagnets [23,24]. Lu et al. synthesized the PANI nanotubes containing Fe_3O_4 NPs under an ultrasonic irradiation condition [25]. At the same time, the synthesis of MWNTs/PANI has also been developed by several groups [26,27]. However, to the best of our knowledge, few reports have studied the 1D nanostructures of PANI coated MWNTs/Fe_3O_4 NPs.

In this paper, we reported a facile method to prepare MWNTs/Fe_3O_4 NPs/PANI composite nanotubes in two steps. The first step was to synthesize nearly monodispersed Fe_3O_4 NPs on the surface of MWNTs by an in situ method, and we could get fine morphology without Fe_3O_4 NPs aggregates even at a high weight ratio of Fe_3O_4 NPs. The second step was to decorate the nanocomposites with PANI via a self-assembly process. In order to prevent the nanostructure of MWNTs/Fe_3O_4 NPs from being destroyed, no kinds of acids were introduced and $FeCl_3$ was used as the oxidant in the second step. It was found that the obtained samples had a nanotubular morphology. TEM images showed that the MWNTs/Fe_3O_4 NPs nanotubes were coated with a thin PANI layer.

2. Experimental

2.1. Materials

Aniline monomer was distilled under reduced pressure and stored below 0 °C before use. MWNTs used in this work were purchased from Shenzhen Nanotech. Port. Co., Ltd. (China). Other reagents were analytical grade and used without further purification including $FeCl_3 \cdot 6H_2O$, $FeCl_2 \cdot 4H_2O$, $NH_3 \cdot H_2O$. The as-prepared MWNTs were treated as follows: 0.1 g of MWNTs was added in a mixture of concentrated nitric acid (10 ml) and sulfuric acid (30 ml) and ultrasonicated over 8 h, then added 90 ml of distilled water into the mixture. It was then centrifuged, washed with distilled water until the dispersion turned neutral, at last dried at 50 °C over night.

2.2. In situ synthesis of MWNTs/Fe_3O_4 NPs nanotubes

Forty-eight mg of functionalized MWNTs were dissolved in 30 ml of distilled water by ultrasonic irradiation for 20 min. Then 40.5 mg of $FeCl_3 \cdot 6H_2O$ was added under stirring. After the mixture was stirred vigorously for 30 min under N_2 atmosphere, 60 mg of $FeCl_2 \cdot 4H_2O$ was added and keep stirring under N_2 atmosphere for 30 min. Four ml of concentrated $NH_3 \cdot H_2O$ diluted with 20 ml of distilled water was added into the mixture drop by drop. The adding of $NH_3 \cdot H_2O$ aqueous solution was finished in 1 h and then the solution was heated to 60 °C and reacted for another 2 h. The whole process must be under N_2 atmosphere. The reaction mixture was then centrifuged, washed with distilled water and dried at 50 °C for 24 h.

2.3. Synthesis of MWNTs/Fe_3O_4 NPs/PANI nanotubes

Seventy mg of MWNTs/Fe_3O_4 NPs nanotubes were dissolved in 30 ml of distilled water by ultrasonic irradiation for 20 min. In a typical procedure, 0.14 g of aniline was added to a 7.5 ml of above solution. The solution was stirred for 30 min and cooled at 0–5 °C for half an hour. Then, 0.408 g of $FeCl_3 \cdot 6H_2O$ in 7.5 ml of distilled water precooled at 0–5 °C was added quickly. The mixture was allowed to react at 0–5 °C for 15 h followed by centrifuged, washed with distilled water and ethanol, dried at 50 °C for 24 h.

2.4. Measurements

Scanning electron microscopy (SEM) measurements were performed on a SHIMADZU SSX-550 microscope equipped with energy dispersive X-ray spectrometry (EDX). Transmission electron microscopy (TEM) experiments were performed on a Hitachi 8100 electron microscope (Tokyo, Japan) and a JEM-2000.EX electron microscope with an acceleration voltage of 200 kV. Fourier transform infrared (FTIR) spectra of KBr powder-pressed pellets were recorded on a BRUKER VECTOR22 spectrometer. Transmission spectra of doped and dedoped MWNTs/Fe_3O_4 NPs/PANI nanotubes were recorded on a Shimadzu UV-3101 PC spectrometer. Raman spectra were recorded on a Renishaw system 1000 spectrometer equipped with an air-cooled CCD detector. The 514.5 nm excitation line used was from an air-cooled argon ion laser. Laser power at the sample stage was about 4 mW. X-ray diffraction (XRD) patterns were obtained with a Siemens D5005 diffractometer using Cu$K\alpha$ radiation. The standard Van Der Pauw DC four-probe method was used to measure the electron transport behavior of PANI nanotubes containing MWNTs/Fe_3O_4 NPs nanocomposites. The samples were pressed into pellet. Then the pellet was cut into a square which was placed on the four-probe apparatus. Providing a voltage, we can obtain the corresponding electrical current. The electrical conductivity was calculated by the following formula: $\sigma\ (S/\mathrm{cm}) = (2.28 \times 10/S) \times (I/E)$, where σ is the conductivity, S is the sample side area, I is the current passed through outer probes, E is the voltage drop across inner probes. The room temperature magnetization in the applied magnetic field was performed by model JDM-13 vibrating sample magnetometer.

3. Results and discussion

3.1. Preparation of MWNTs/Fe_3O_4 NPs/PANI nanocomposites

The preparation process of MWNTs/Fe_3O_4 NPs/PANI nanotubes is illustrated in Scheme 1. As it shows, acid-treated MWNTs are functionalized with negative carboxylic groups which have affinity with positive ferrous

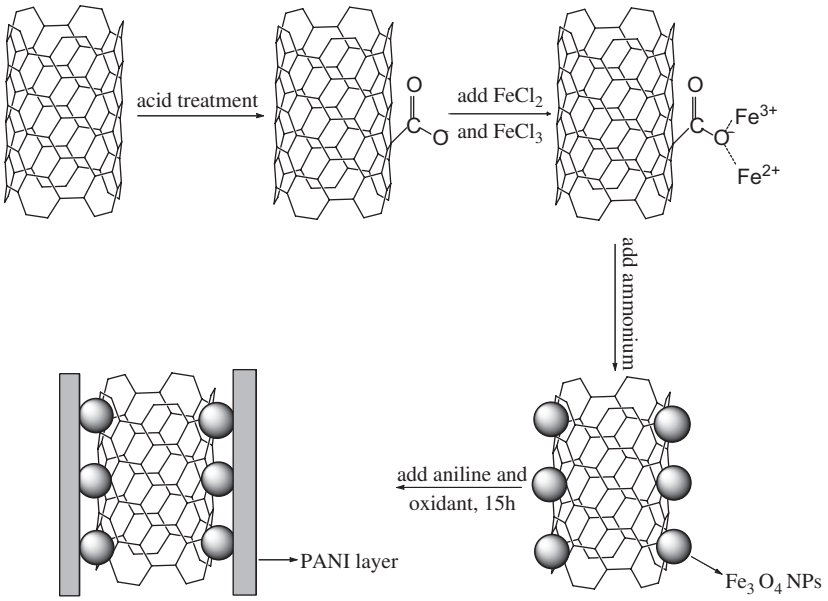

Scheme 1. Simplified schematic representation of the preparation of MWMTs/Fe_3O_4 NPs/PANI nanotubes by a two-step method.

and ferric ions. After the addition of $NH_3 \cdot H_2O$ aqueous solution, Fe_3O_4 NPs will be formed on the surface of MWNTs. The weight ratio of Fe_3O_4 NPs can be controlled by changing the amount of added $FeCl_3 \cdot 6H_2O$ and $FeCl_2 \cdot 4H_2O$. Fe_3O_4 NPs aggregates will appear if the adding amount of $FeCl_3 \cdot 6H_2O$ is more than 54 mg and that of $FeCl_2 \cdot 4H_2O$ is more than 80 mg. From our experiments, it was found that the ultrasonic irradiation time of functionalized MWNTs before stirring had a great effect on the morphology of MWNTs/Fe_3O_4 NPs nanotubes and 15–20 min would be appropriate. Large Fe_3O_4 NPs aggregates would appear if we reduced the ultrasonic irradiation time to less than 5 min, but there was not much change when the ultrasonic irradiation time was prolonged to more than half an hour. Then we coated the nanocomposites with PANI layer through a self-assembly method. We have tried to use several methods to prepare the MWNTs/Fe_3O_4 NPs/PANI nanocomposites in acidic solution but failed. There were always large Fe_3O_4 NPs aggregates in PANI layer and bare MWNTs. We concluded from these failures that acidic solution may destroy the attachment between Fe_3O_4 NPs and MWNTs, so we chose to experiment without adding any acids. However, when we use the ammonium peroxydisulfate (APS) as the oxidant, the morphology of 1D nanocomposite could not be obtained. Ding et al. reported the controlling of diameters of PANI nanotubes by adjusting the oxidant redox potential [28]. When they used $FeCl_3$ with a low redox potential of 0.77 V as the oxidant, the diameter of prepared PANI nanotubes was 18 nm. In this process, aniline showed oxidation potentials of 0.45 V [31]. So we tried to use $FeCl_3$ as the oxidant. At last, the samples with nanotubular morphology are obtained and their diameters were about 100–150 nm.

3.2. Morphology of MWMTs/Fe_3O_4 NPs/PANI nanotubes

SEM images showed that the resulting samples have the morphology of nanotubes and these nanotubes were obviously different from MWNTs (Fig. 1). First, the surface of nanocomposites was rough while the surface of MWNTs was smooth. Second, the diameter of MWNTs/Fe_3O_4 NPs/PANI nanotubes was about 100–150 nm but that of MWNTs was about 60–100 nm. From the TEM images (Fig. 2), it could be clearly seen that Fe_3O_4 NPs with an average diameter of 17.6 nm ($\sigma = 1.92$ nm) were attached to MWNTs and a PANI layer was coated on the surface of MWNTs/Fe_3O_4 NPs nanocomposites.

We have also changed the molar ratio of $FeCl_3$ to aniline and the molar concentration of aniline to investigate the best conditions for preparing MWNTs/Fe_3O_4 NPs/PANI nanotubes. First, we changed the molar ratio of $FeCl_3$ to aniline from 8:1 to 0.5:1. As can be seen from the SEM images (Fig. 3), 2:1 would be the proper ratio for the synthesis of multifunctional composite nanotubes. Amplify or reduce the ratio would only get samples with PANI aggregates. From the TEM images, when the ratio was 8:1, MWNTs was coated with a thick layer of PANI and there were still dissociative PANI in the final product. After the ratio was lowed to 4:1, thin PANI nanofibers were grown onto MWNTs. This is due to the high rate of aniline polymerization. On the other hand, when the ratio was lowed to less than 2:1, we could hardly see any PANI coated MWNTs/Fe_3O_4 NPs. After we fixed the appropriate molar ratio, we changed the molar concentration of aniline from 0.2 to 0.025 M. It could be clearly seen from the SEM and TEM images (Fig. 4) that the proper concentration of aniline was 0.1 M. There would also be PANI aggregates and the PANI layer onto MWNTs/Fe_3O_4 NPs was too

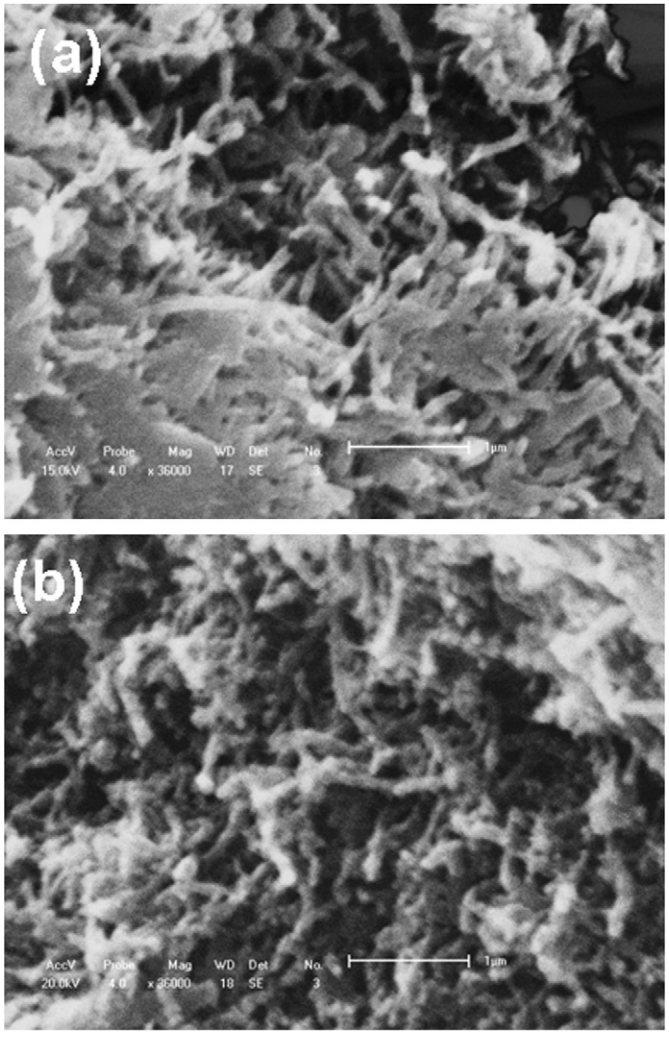

Fig. 1. SEM images of (a) MWNTs and (b) MWNTs/Fe_3O_4 NPs/PANI nanocomposites. Synthetic conditions of MWNTs/Fe_3O_4 NPs/PANI nanocomposites: $FeCl_3$:Aniline = 2:1, [An] = 0.1 mol/L, T = 0–5 °C, t = 15 h.

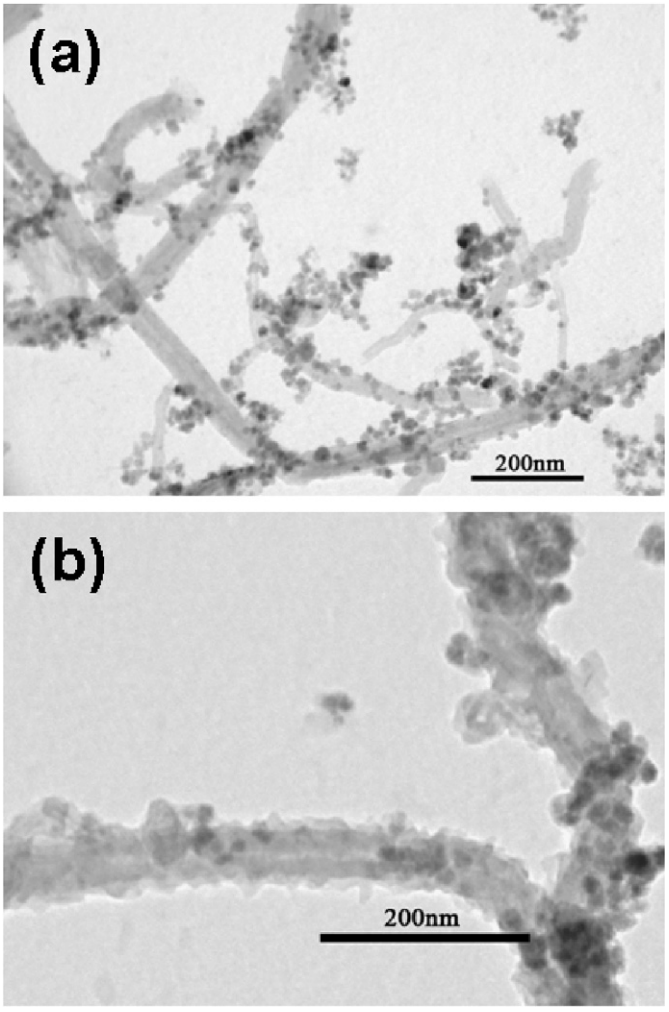

Fig. 2. TEM images of (a) MWNTs/Fe_3O_4 NPs composites; (b) MWNTs/Fe_3O_4 NPs/PANI nanocomposites. Synthetic conditions of MWNTs/Fe_3O_4 NPs/PANI nanocomposites: $FeCl_3$:Aniline = 2:1, [An] = 0.1 mol/L, T = 0–5 °C, t = 15 h.

thick when the concentration was higher than 0.2 M. On the other hand, when we decreased it to 0.05 M or lower, few MWNTs/Fe_3O_4 NPs nanocomposites could be coated with PANI layer.

3.3. Structural characterization of MWMTs/Fe_3O_4 NPs/PANI nanotubes

FTIR were used to characterize the molecular structure of MWMTs/Fe_3O_4 NPs/PANI composite nanotubes. Fig. 5 shows the characteristic peaks of functionalized MWNTs, MWMTs/Fe_3O_4 NPs nanotubes, PANI nanotubes and MWMTs/Fe_3O_4 NPs/PANI nanotubes. It was found that MWMTs/Fe_3O_4 NPs/PANI nanotubes had characteristic peaks at around 3428 cm^{-1} (N–H stretching), 1571 cm^{-1}, 1493 cm^{-1} (C═C stretching deformation of quinoid and benzenoid ring, respectively), 1304 cm^{-1} (C–N stretching of secondary aromatic amine), 1123 cm^{-1} and 821 cm^{-1} (out-of-plane deformation of C–H in the 1,4-disubtituted benzene ring), which is similar with that of PANI sample [29]. From the IR spectrum of MWMTs/Fe_3O_4 NPs nanotubes, we cannot find the characteristic peaks of PANI while the peak at about 3430 cm^{-1} is due to the crystal water.

Fig. 6 displays the EDX spectra for MWMTs/Fe_3O_4 NPs/PANI nanotubes. From this spectrum, we can find C peak at 0.24 keV, O peak at 0.52 keV, Fe peak at 0.69 and 6.41 keV and Cl peak at 2.61 keV. As the PANI layer is very thin, N peak cannot be clearly seen from EDX spectra. As a result, we use XPS spectrum which is more precise to confirm the existence of N element (Fig. 7). The N1s core-level spectra of the nanocomposites have been deconvoluted by assigning binding energies of 398.6, 399.5, and 400.6 eV for the imine (–N═), amine (–NH–), and polaron species (N^+), respectively. Note that the second component peak (amine site) is dominant in the N1s core-level spectrum as PANI is not in its doped state. Besides N, we can also find other four elements from the spectrum and

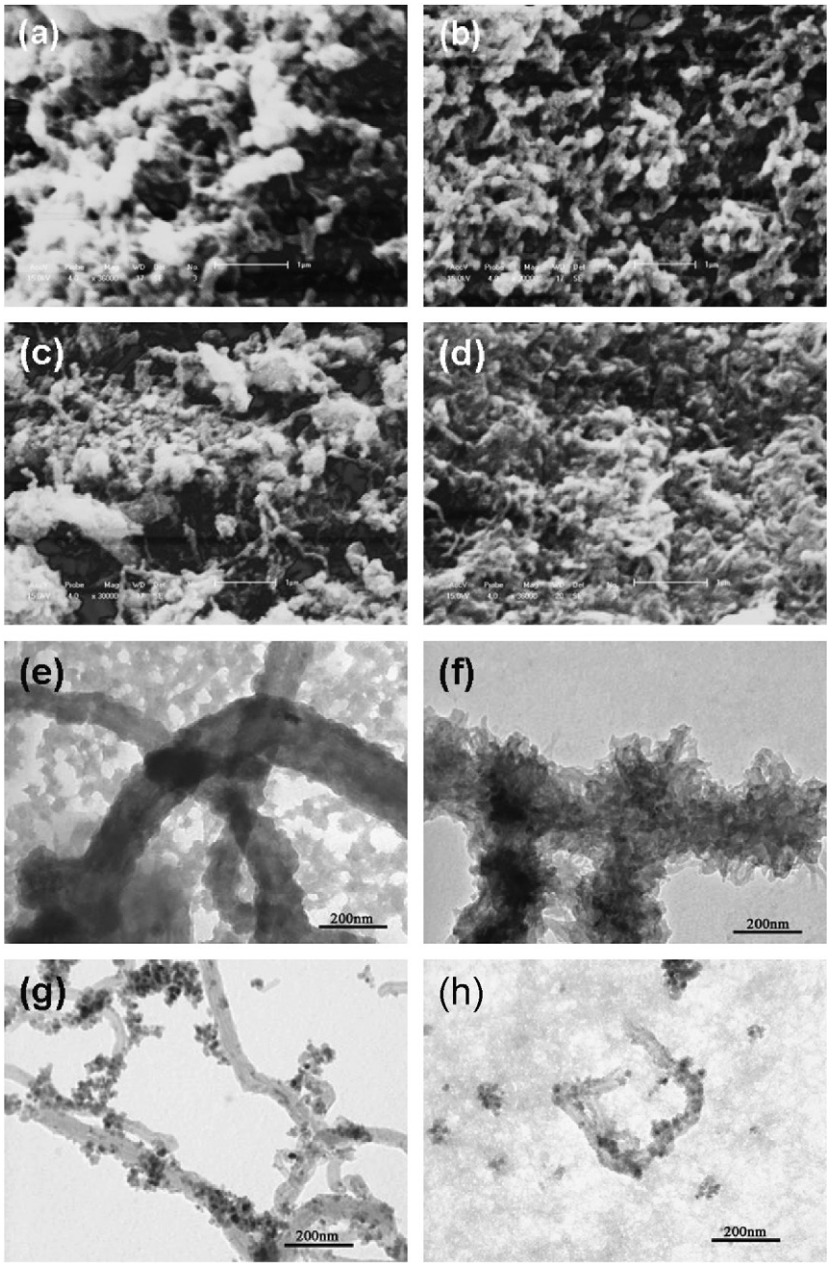

Fig. 3. SEM images of MWNTs/Fe_3O_4 NPs/PANI samples using different ratios of $FeCl_3$ to Aniline: (a) 8:1; (b) 4:1; (c) 1:1; (d) 0.5:1. TEM images of MWNTs/Fe_3O_4 NPs/PANI samples using different ratios of $FeCl_3$ to Aniline: (e) 8:1; (f) 4:1; (g) 1:1; (h) 0.5:1. Other conditions: [An] = 0.1 mol/L, $T = 0$–$5\,^{\circ}C$, $t = 15$ h.

the weight ratios are: C, 78.00%; N, 3.79%; O, 13.32%; Fe, 3.85%; Cl, 1.02%.

The XRD patterns of samples are shown in Fig. 8. The diffraction of the Fe_3O_4 NPs are observed in MWMTs/Fe_3O_4 NPs/PANI nanotubes and MWMTs/Fe_3O_4 NPs nanotubes, including the peaks at $2\theta = 29.95^{\circ}$, 35.45°, 43.1°, 57.25° and 62.8°. These data are in good agreement with that of Fe_3O_4 NPs reported before [30]. The nanocomposites also contained the characteristic peaks of MWNTs at $2\theta = 26.2^{\circ}$ and 44.4°. These data showed the existence of MWNTs, Fe_3O_4 NPs in the nanocomposites. As PANI is not crystalline, we cannot make sure of its existence from XRD patterns.

At the same time, the results of Raman spectra (Fig. 9) further confirm the formation of PANI on MWNTs. For comparison, this figure also includes the spectra of pure MWNTs, acid-treated MWNTs and MWNTs/Fe_3O_4 NPs nanotubes. The patterns of pure MWNTs, acid-treated MWNTs and MWNTs/Fe_3O_4 NPs nanotubes indicate that the surface modification does not affect the graphite structure of MWNTs. Two strong peaks at $1583\,cm^{-1}$ (G mode) which is the Raman allowed phonon high-frequency mode and a disordered peak at $1351\,cm^{-1}$ (D mode) which may originate from the defects in the curved graphite sheets and tube ends. But, these two peaks are lower in MWNTs/Fe_3O_4 NPs/PANI nanocomposites. For

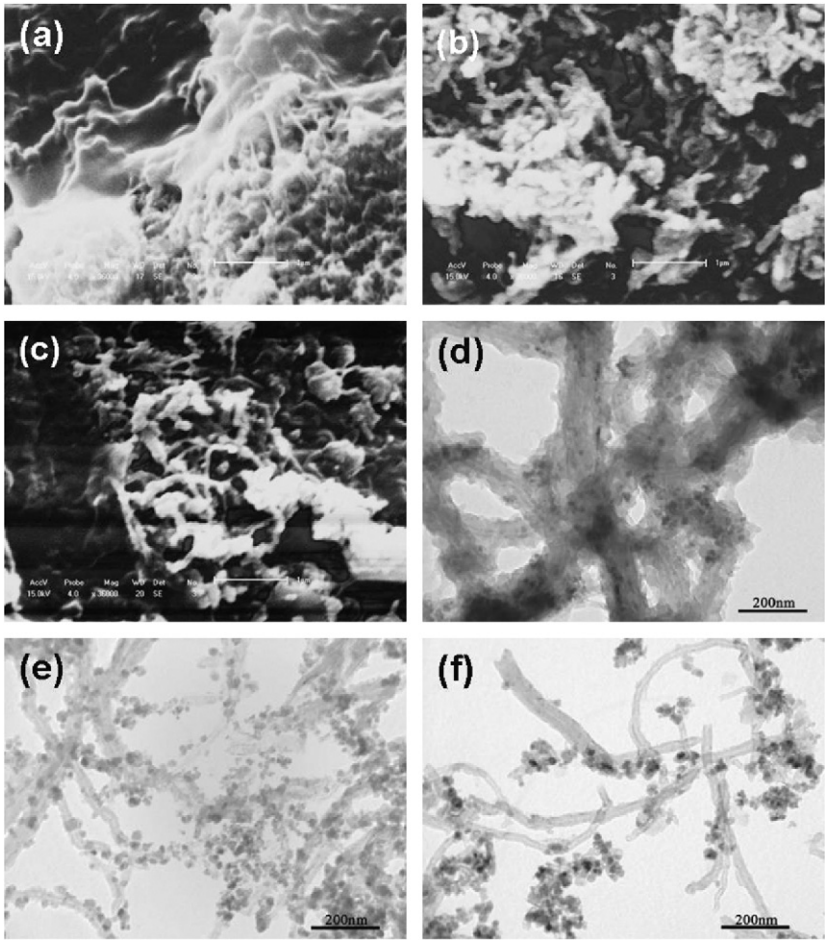

Fig. 4. SEM images of MWNTs/Fe_3O_4 NPs/PANI samples using different Aniline concentrations: (a) 0.2 mol/L; (b) 0.05 mol/L; (c) 0.025 mol/L. TEM images of MWNTs/Fe_3O_4 NPs/PANI samples using different Aniline concentrations: (d) 0.2 mol/L; (e) 0.05 mol/L; (f)0.025 mol/L. Other conditions: $FeCl_3$:Aniline = 2:1, $T = 0$–5 °C, $t = 15$ h.

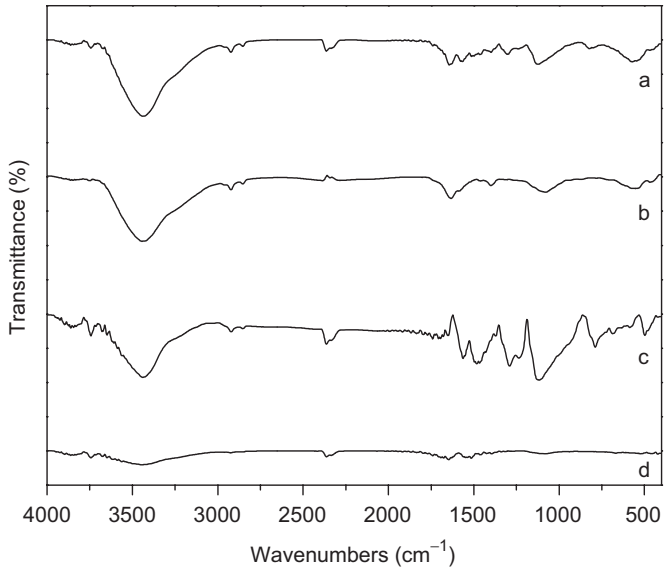

Fig. 5. The IR spectra of (a) MWNTs/Fe_3O_4 NPs/PANI nanocomposites; (b) MWNTs/Fe_3O_4 NPs nanocomposites; (c)PANI; (d) acid-treated MWNTs.

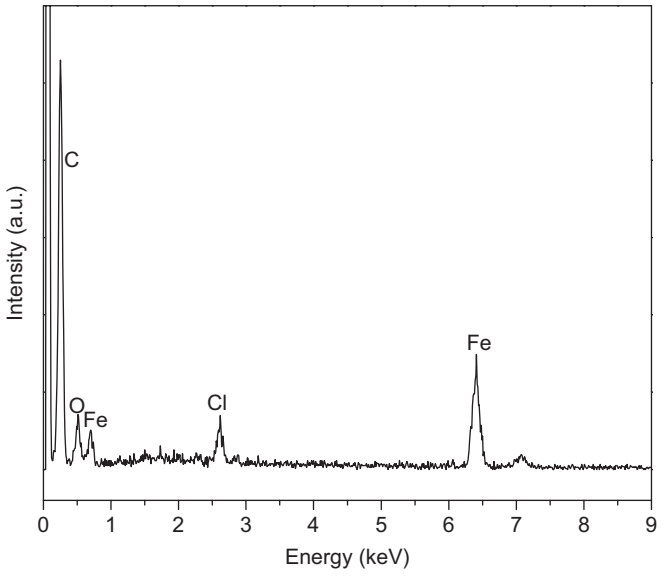

Fig. 6. The EDX spectra of MWNTs/Fe_3O_4 NPs/PANI nanocomposites.

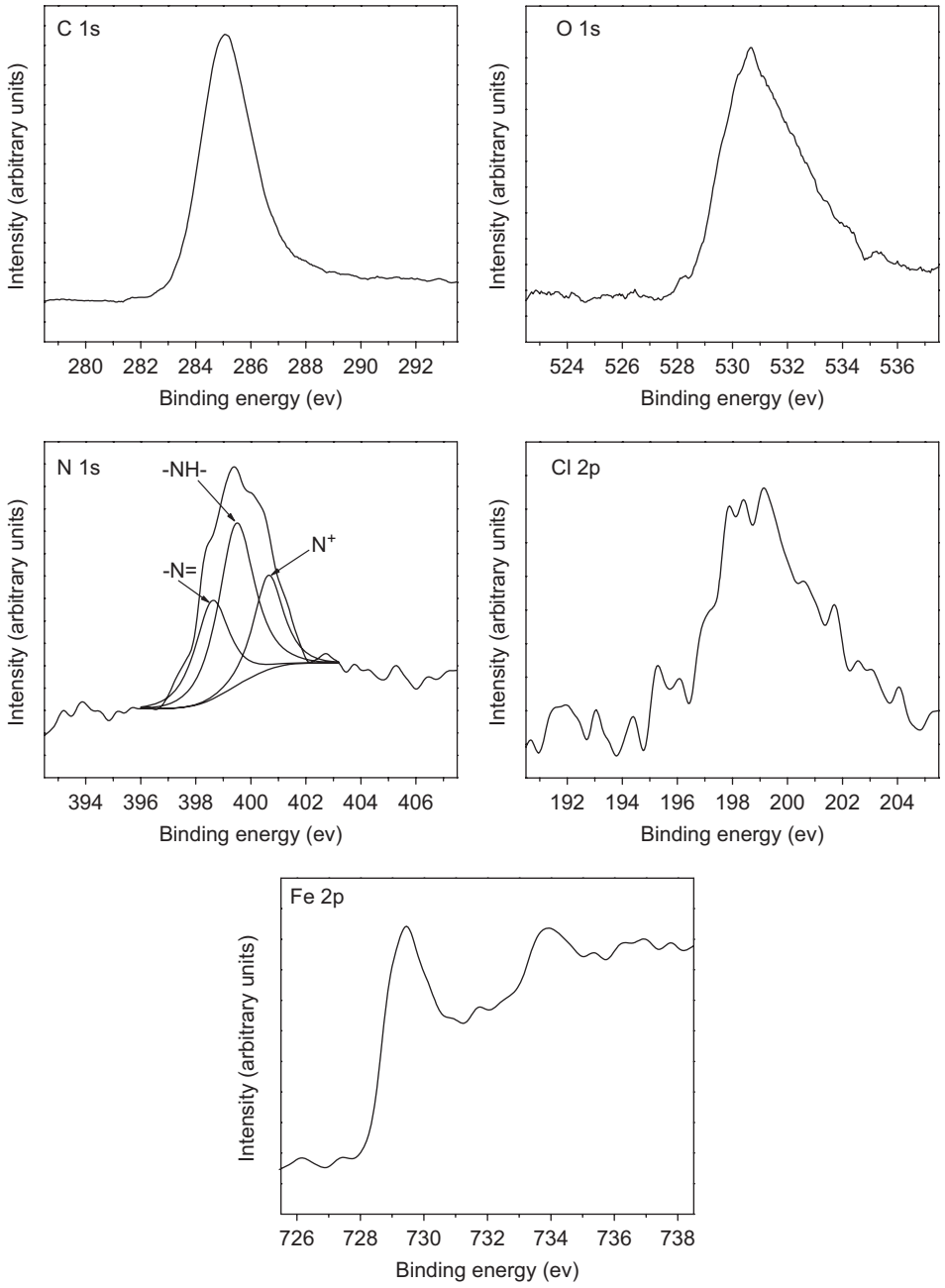

Fig. 7. The XPS spectrum of MWNTs/Fe_3O_4 NPs/PANI nanocomposites.

MWNTs/Fe_3O_4 NPs/PANI nanocomposites, C–H bending of the quinoid ring at 1162 cm^{-1}, electronic absorption of free charge carriers at 1404 cm^{-1}, N–H bending at 1497 cm^{-1}, C–C stretching of benzene ring at 1618 cm^{-1} are observed while C–N^+ at 1334 cm^{-1} cannot be seen from the spectra. These differences reveal that PANI film is present on the MWNTs/Fe_3O_4 NPs surface and PANI is not in its doped state [32,33].

UV–vis spectra of MWMTs/Fe_3O_4 NPs/PANI nanotubes in neutral solution, doped and dedoped MWMTs/Fe_3O_4 NPs/PANI nanotubes dispersed in distilled water are shown in Fig. 10. In order to verify that the nanocomposites can respond to acid and alkali, we separately dispersed a part of the sample in 5 mol/L HCl aqueous solution, neutral solution and 5 mol/L $NH_3 \cdot H_2O$ aqueous solution . From the transmission spectra of doped nanocomposites, we find that the characteristic peaks of acid-treated PANI at 280–340 nm (π–π^* transition), 400–450 nm (polaron–π^* transition), 780–900 nm (π–polaron transition) are observed. As the PH increases, the peak at 280–340 nm is much lower and there appears a new peak at about 550–600 nm, this is due to the conjugated quinoid diimino group of PANI in its emeraldine base state. From these data, it is concluded that the nanocomposites can well respond to acid and alkali.

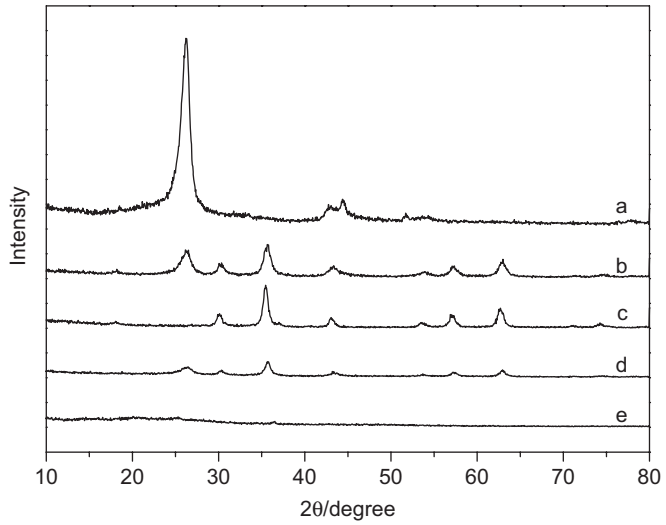

Fig. 8. XRD scattering patterns of: (a) MWNTs; (b) MWNTs/Fe_3O_4 NPs nanocomposites; (c) Fe_3O_4 NPs; (d) MWNTs/Fe_3O_4 NPs/PANI nanocomposites; (e) PANI.

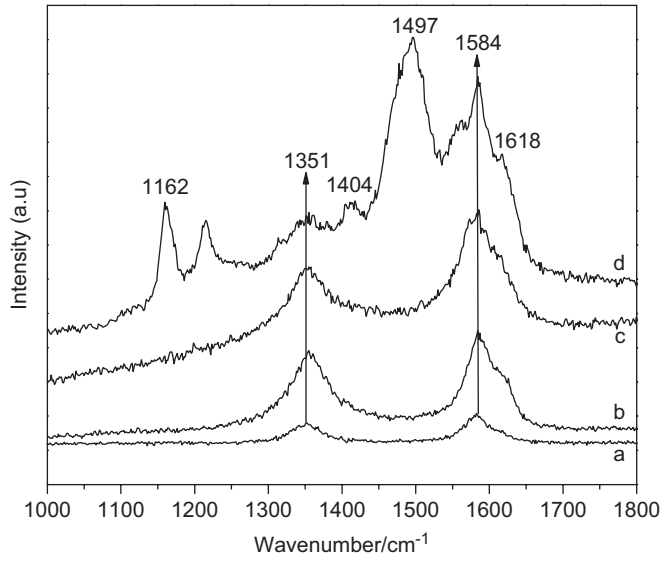

Fig. 9. Raman spectra of (a) MWNTs; (b) acid-treated MWNTs; (c) MWNTs/Fe_3O_4 NPs nanocomposites; (d) MWNTs/Fe_3O_4 NPs/PANI nanocomposites.

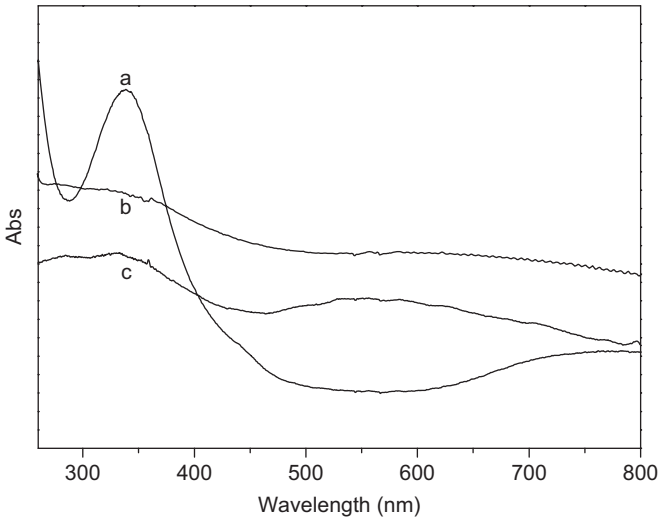

Fig. 10. UV–vis spectra of (a) doped MWNTs/Fe_3O_4 NPs/PANI nanocomposites; (b) MWNTs/Fe_3O_4 NPs/PANI nanocomposites in neutral solution; (c) dedoped MWNTs/Fe_3O_4 NPs/PANI nanocomposites.

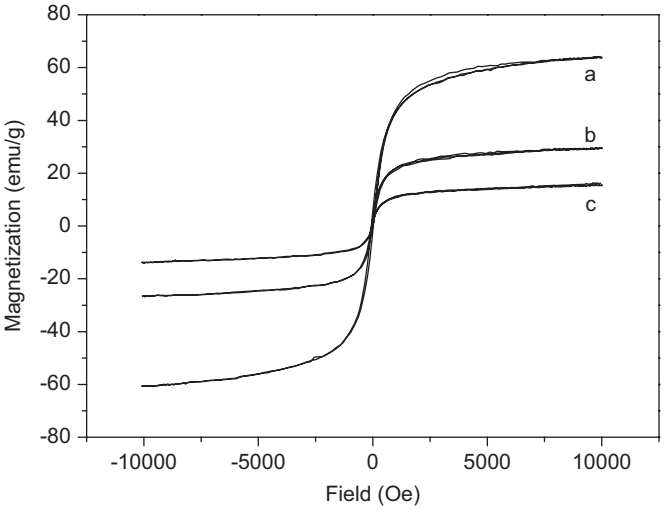

Fig. 11. Magnetization vs. applied magnetic field at room temperature for: (a) Fe_3O_4 nanoparticles and (b) MWNTs/Fe_3O_4 NPs nanocomposites and (c) MWNTs/Fe_3O_4 NPs/PANI nanocomposites.

The conductivities of the resulted MWMTs/Fe_3O_4 NPs/PANI composite nanotubes and MWMTs/Fe_3O_4 NPs nanotubes are measured by the standard Van Der Pauw DC four-probe method. It is found that the conductivities of MWMTs/Fe_3O_4 NPs nanotubes are 3.17×10^{-6} S/cm due to the high weight ratio of Fe_3O_4 NPs. After the coating of PANI layer, the conductivities changed to 4.22×10^{-6} S/cm, which does not increased much. This is probably due to the lower doping level because of no acids were used in the experiment. The magnetic properties of obtained nanotubes are investigated with a vibrating sample magnetometer. Typical magnetization curves as a function of applied field at room temperature (300 K) are shown in Fig. 11. There is no pronounced hysteresis loop, which indicates that both the retentivity and the coercivity of the composites are zero. This observation is consistent with superparamagnetic behavior. As shown in Fig. 11, the MWMTs/Fe_3O_4 NPs nanotubes have a saturated magnetization of $M_s = 29.4$ emu/g and the MWMTs/Fe_3O_4 NPs/PANI nanotubes have a saturated magnetization of $M_s = 15.8$ emu/g. The difference between their saturated magnetizations is due to the different weight ratios of Fe_3O_4 NPs.

4. Conclusions

In summary, we reported a facile method to prepare magnetic and conductive MWMTs/Fe_3O_4 NPs/PANI

composite nanotubes through a two-step process. We first in situ synthesize Fe_3O_4 NPs on the surface of MWNTs and then coated the nanocomposites with PANI layer via a self-assembly method using $FeCl_3$ as the oxidant. SEM and TEM images confirmed the core-sheath nanostructure and the attachment of Fe_3O_4 NPs on the surface of MWNTs. The effect of the molar ratio of $FeCl_3$ to aniline and the concentration of aniline to the morphologies of the obtained composite was investigated. FTIR and XRD spectra were used to characterize the molecular structure of the nanocomposites. UV–vis spectra showed that the obtained nanotubes could respond to both acid and alkali. The conductivity and magnetization measurements proved that the samples are conductive and have a superparamagnetic behavior.

Acknowledgments

The financial support from the National Natural Science Foundation of China (NNSFC-20674027) and the National Major Project for Fundamental Research of China (National 973 Program No. G2003CB615604) is greatly appreciated.

References

[1] S. Iijima, Nature 354 (1991) 56.
[2] [2a] J.W.G. Wilder, L.C. Venema, A.G. Rinzler, R.E. Smalley, C. Dekker, Nature (London) 391 (1998) 59;
[2b] T.W. Odom, J.L. Huang, P. Kim, C.M. Lieber, Nature (London) 391 (1998) 62.
[3] M.M.J. Treacy, T.W. Ebbesen, J.M. Gibson, Nature (London) 381 (1996) 678.
[4] M.J. O'Connell, S.M. Bachilo, C.B. Huffman, V.C. Moore, M.S. Strano, E.H. Haroz, K.L. Rialon, P.J. Boul, W.H. Noon, C. Kittrell, J. Ma, R.H. Hauge, R.B. Weisman, R.E. Smalley, Science 297 (2002) 593.
[5] T.W. Odon, J. Huang, P. Kim, C.M. Lieber, Nature (London) 391 (1998) 62.
[6] B. Kim, W.M. Sigmund, Langmuir 20 (2004) 8239.
[7] C.S. Li, Y.P. Tang, K.F. Yao, Carbon 44 (2006) 2021.
[8] L.T. Qu, L.M. Dai, E.J. Osawa, J. Am. Chem. Soc. 128 (2006) 5523.
[9] Y. Shan, L. Gao, Mater. Chem. Phys. 103 (2007) 206.
[10] K.Y. Jiang, A. Eitan, L.S. Schadler, Nano lett. 3 (2003) 275.
[11] X.G. Hu, T. Wang, X.H. Qu, J. Phys. Chem. B 110 (2006) 853.
[12] X.G. Hu, T. Wang, L. Wang, Langmuir 23 (2007) 6352.
[13] J.L. Dormann, D. Fioranim, Magnetic Properties of Fine Particles, North-Holland, Amsterdam, 1991, p. 309.
[14] C.M. Wang, Z. Wang, M.K. Li, Chem. Phys. Lett. 341 (2001) 431.
[15] H.J. Qiu, M.X. Wan, J. Polym. Sci. Part A: Polym. Chem. 39 (2001) 3485.
[16] D.H. Reneker, I. Chun, Nanotechnology 7 (1996) 216.
[17] L.J. Zhang, M.X. Wan, Thin Solid Films 477 (2005) 24.
[18] Z.X. Wei, Z.M. Zhang, M.X. Wan, Langmuir 18 (2002) 917.
[19] J. Huang, S. Virji, B.H. Weiller, R.B. Kaner, J. Am. Chem. Soc. 125 (2003) 314.
[20] X.F. Lu, Y.H. Yu, L. Chen, H.P. Mao, L.F. Wang, W.J. Zhang, Y. Wei, Polymer 46 (2005) 5329.
[21] J.Q. Wan, W. Cai, J.T. Feng, J. Mater. Chem. 17 (2007) 1188.
[22] M.A. Correa-Duarte, M. Grzelczak, V. Salgueirino-Maceira, J. Phys. Chem. B 109 (2005) 19060.
[23] Y.Z. Long, Z.J. Chen, Z.X. Liu, Chin. Phys. 12 (2003) 433.
[24] Z.M. Zhang, M.X. Wan, Synth. Met. 132 (2003) 205.
[25] X.F. Lu, H. Mao, D.M. Chao, W.J. Zhang, Y. Wei, J. Solid State Chem. 179 (2006) 2609.
[26] B.J. Philip, J.N. Xie, J.K. Abraham, Polym. Bull. 53 (2005) 127.
[27] Y.J. Yu, B. Che, Z.H. Si, Synth. Met. 150 (2005) 271.
[28] H.J. Ding, M.X. Wan, Y. Wei, Adv. Mater. 19 (2007) 465.
[29] X. Lu, Y. Yu, L. Chen, H. Mao, W. Zhang, Y. Wei, Chem. Commun. (2004) 1522.
[30] X. Lu, Y. Yu, L. Chen, H.P. Mao, H. Gao, J. Wang, W.J. Zhang, Y. Wei, Nanotechnology 16 (2005) 1660.
[31] C. Jose, M. Vanessa, H. Rafael, P. Charlotte, Electrochim. Acta 44 (1999) 2507.
[32] Z.J. Wang, J.H. Yuan, M.Y. Li, D.X. Han, Y.J. Zhang, N. Liu, J. Electroanal. Chem. 599 (2007) 121.
[33] Z.X. Wei, Z.M. Zhang, M.X. Wan, Langmuir 18 (2002) 917.